

## Sol-gel synthesis, Structural and Infrared Properties of Zinc Substituted $\text{Co}_{1-x}\text{Zn}_x\text{Fe}_2\text{O}_4$ ( $x = 0.2, 0.6$ and $1.0$ ) Nanoparticles

SWATI B. KALE<sup>1\*</sup>, M. K. BABREKAR<sup>2</sup>, DILIP R. SAPATE<sup>3</sup>, K. M. JADHAV<sup>4</sup>

<sup>1</sup>Dept. of Applied Sciences, Government Polytechnic, Aurangabad – 431001 (M.S.), India

<sup>2</sup>Dept. of Physics, Indraraj College, Sillod, Aurangabad, (M.S.), India

<sup>3</sup>Dept. of Physics, Sant Ramdas College, Ghansawangi, Jalna (M.S.), India

<sup>4</sup>Dept. of Physics, Dr. Babasaheb Ambedkar Marathwada University, Aurangabad (M.S.), 431004, India

\* Corresponding author E-mail: sbkale14@gmail.com

doi: 10.30731/ijcps.7.2.2018.97-102

### Abstract

*In the present work, sol-gel synthesis, structural and infrared properties of zinc substituted cobalt ferrite nanoparticles was reported. Zinc substituted cobalt ferrite ( $\text{Co}_{1-x}\text{Zn}_x\text{Fe}_2\text{O}_4$ ,  $x = 0.2, 0.6$  and  $1.0$ ) have been prepared using sol-gel auto combustion method by taking citric acid as a fuel. The metal nitrate to fuel ratio was taken as 1:3 as per stoichiometric proportions. The obtained nanoparticles were characterized by X-ray diffraction method and infrared spectroscopy. X-ray diffraction pattern (XRD) recorded at 300 K shows well defined Bragg's reflections belonging to cubic spinel structure. The XRD pattern analysis clearly shows the formation of single phase cubic spinel structure as well as nanocrystalline behaviour of the prepared samples. The average crystallite size calculated using Scherrer's formula is found to be in the range 18 to 21 nm. The lattice constant found to be increase for higher zinc composition  $x$ . Using XRD data, various structural parameters such as dislocation density, X-ray density, bulk density, porosity etc. were calculated. The room temperature IR spectra revealed the presence of two absorption bands approximately near to  $400\text{ cm}^{-1}$  and  $600\text{ cm}^{-1}$  showing characteristics feature of spinel ferrite which can be attributed to tetrahedral (A) and octahedral [B] metal stretching.*

**Keywords:** Co-Zn nanoparticles; Sol-gel auto combustion; XRD; Infrared

### Introduction

Nanostructured materials are considered very attractive as compared to their bulk counterpart as they exhibit advanced physical and chemical properties because of the quantum confinement, smaller size (nm dimension), high surface area etc [1, 2]. The synthesis of new materials at nanoscale level is attracting the great attention of scientist and technologist from last decade. The size, shape and purity of the nanostructured materials are more important to modify the properties for desired applications [3]. Spinel ferrites crowned by the formula  $\text{AFe}_2\text{O}_4$ , where A is a divalent cation like Co, Zn, Cu, Mg etc. are one of the most attractive magnetic nanoparticles due to their applications in diverse fields [4]. The properties of spinel ferrites are strongly prejudiced by the materials composition, microstructure, type of dopant, amount of dopant, cation distribution etc. Synthesis of nanoparticles is an exciting and demanding area of research for the technological and biomedical applications [5]. Many synthesis methods have been developed by the research community for the synthesis of spinel ferrite nanoparticles such as ball milling, sonochemical, sol-gel, chemical coprecipitation, hydrothermal etc [6, 7].

Among the spinel ferrite,  $\text{CoFe}_2\text{O}_4$  is a partially inverse spinel ferrite in which  $\text{Co}^{2+}$  ions occupy the octahedral B-sites and  $\text{Fe}^{3+}$  ions occupy both tetrahedral A-site and octahedral B-site and its degree of inversion is sensitive to the thermal history of the sample, microstructure and preparative parameters. Cobalt ferrites have been extensively used in microelectronic devices because of their large permeability at high frequency, high electrical resistivity, high saturation magnetization, mechanical hardness, chemical stability and cost effectiveness [8]. In addition to pure cobalt ferrite nanoparticles, divalent metal ion substituted cobalt ferrites are widely studied by researchers for various applications.

Zinc (Zn) substitution plays a vital role in determining the variety of properties of cobalt ferrites. Mixed Zn ferrites and especially zinc substitutes cobalt ferrites are the most important magnetic materials. Zn substitution in cobalt ferrite results in dilution of the magnetic lattice although there is a decrease in the magnetostriction it was observed that the slope of magnetostriction could be enhanced due to reduction in magnetic anisotropy [9].

It will be more interested to study the effect of zinc substitution on structural and infrared properties of cobalt spinel ferrite nanoparticles. Thus, we report here the sol-gel synthesis, structural and infrared properties of Zn substituted cobalt ferrite ( $\text{Co}_{1-x}\text{Zn}_x\text{Fe}_2\text{O}_4$ ,  $x = 0.2, 0.6$  and  $1.0$ ) nanoparticles.

## Experimental Work

### Material and Methods

Cobalt nitrate ( $\text{Co}(\text{NO}_3)_2 \cdot 6\text{H}_2\text{O}$ ), zinc nitrate ( $\text{Zn}(\text{NO}_3)_2 \cdot 6\text{H}_2\text{O}$ ), ferric nitrate ( $\text{Fe}(\text{NO}_3)_3 \cdot 9\text{H}_2\text{O}$ ) and citric acid ( $\text{C}_6\text{H}_8\text{O}_7 \cdot \text{H}_2\text{O}$ ) were used as a raw materials for sol-gel auto combustion synthesis of  $\text{Co}_{1-x}\text{Zn}_x\text{Fe}_2\text{O}_4$  ( $x = 0.2, 0.6$  and  $1.0$ ) spinel ferrite nanoparticles. All the reagents used for the synthesis of Co-Zn ferrite nanoparticles were analytical grade (AR) and used as received without further purification.

$\text{Co}_{1-x}\text{Zn}_x\text{Fe}_2\text{O}_4$  ( $x = 0.2, 0.6$  and  $1.0$ ) nanoparticles were synthesized by sol-gel auto combustion method using citric acid as a fuel. The stoichiometric proportions of metal nitrates to fuel (citric acid) ratio as 1:3 were taken into separate glass beakers. The mixed solution was stirred for 25-30 minutes to dissolve it completely into distilled water. After complete dissolution they were mixed together. Ammonia was added drop by drop into the solution to set pH value at 7. Then the neutralized solution was constantly magnetically stirred and heated at  $100^\circ\text{C}$  for 6 h on a hot plate. On the formation of sol-gel, very viscous gel the temperature was further raised up to  $110^\circ\text{C}$  so that the ignition of the dried gel started and finally powder was obtained. The as prepared loose cobalt ferrite powder was grinded for 30 minutes and annealed at  $550^\circ\text{C}$  for 4 h in muffle furnace.

### Characterizations

X-ray diffraction (XRD) patterns of all the samples were recorded at 300 K by using a PANalytical X'pert pro diffractometer. The diffraction pattern were recorded in the  $2\theta$  range  $20^\circ$  to  $80^\circ$  with scanning rate of  $2^\circ$  per minute using  $\text{Cu-K}_\alpha$  radiation with wavelength of the order of  $1.5406 \text{ \AA}$ . Various structural parameters such as lattice constant, particle size, dislocation density, X-ray density, bulk density and porosity were calculated from the XRD data. The infrared spectra of all the samples were recorded at room temperature in the range  $400 \text{ cm}^{-1} - 1000 \text{ cm}^{-1}$  on FTIR-6100 type-A spectrometer.

## Results and Discussions

### X-ray diffraction (XRD) studies

The fig. 1 (a-c) depicts the XRD patterns of  $\text{Co}_{1-x}\text{Zn}_x\text{Fe}_2\text{O}_4$  ( $x = 0.2, 0.6$  and  $1.0$ ) nanoparticles. The reflections plane indexed (220), (311), (222), (400), (422), (511) and (440) for all the compositions were observed in fig. 1 (a-c). The attendance of all the reflection peaks in the XRD pattern proves the formation of single phase cubic spinel structure. All the peaks in the XRD pattern are sharp and intense. No additional peak other than mentioned above was observed in XRD patterns. This indicates the high purity of prepared samples. Similar XRD pattern for cobalt-zinc ferrite samples was reported in the literature [10].

### Lattice constant ( $a$ )

Using the values of Bragg's angle  $2\theta$  and interplanar spacing  $d$ , the values of lattice constant for all the composition are calculated using the following relation,

$$a = d\sqrt{h^2 + k^2 + l^2} \text{ \AA} \quad \dots 1$$

The values of lattice constant are presented in table 1 and were found to be in the range of  $8.38 \text{ \AA}$  to  $8.44 \text{ \AA}$ . It is observed from table that lattice constant increases with increase in Zn composition  $x$ . The variation of lattice parameter with zinc composition  $x$  could be attributed to the incorporation of  $\text{Zn}^{2+}$  ions of large radius ( $0.82 \text{ \AA}$ ) in place of cobalt ions of small radius ( $0.74 \text{ \AA}$ ). This behaviour of lattice constant is similar to the cobalt-zinc nanoparticles synthesized by other methods and other zinc substituted spinel ferrite [11].

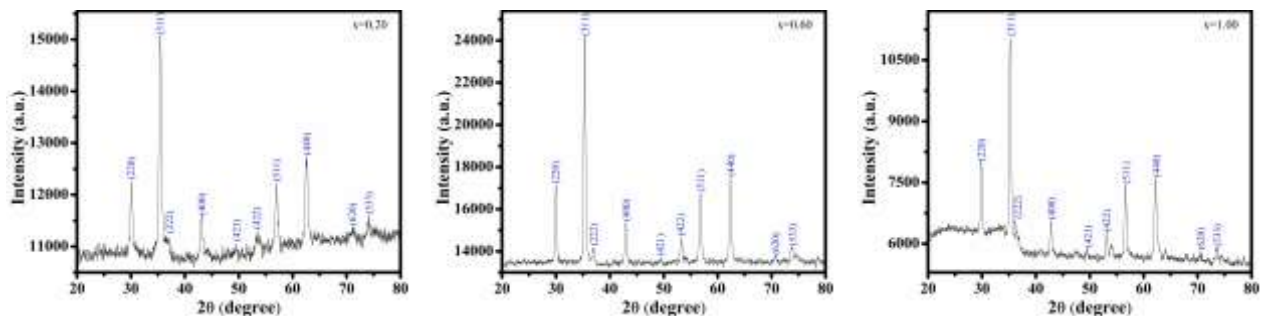


**Fig. 1 (a-c):** X-ray diffraction pattern of  $\text{Co}_{1-x}\text{Zn}_x\text{Fe}_2\text{O}_4$  ( $x = 0.2, 0.6$  and  $1.0$ ) nanoparticles

### Crystallite size ( $t$ )

The crystallite size ( $t$ ) was calculated from the most intense peak (311) present in the XRD patterns using the well known Scherrer's formula,

$$t = \frac{0.9\lambda}{\beta \cos\theta} \text{ nm} \quad \dots 2$$

The crystallite size calculated using the above relation is presented in table 1. The particle sizes of the prepared samples were found to be between 18 nm to 21 nm.

### Dislocation density ( $\delta$ )

The dislocation density ( $\delta$ ) of  $\text{Co}_{1-x}\text{Zn}_x\text{Fe}_2\text{O}_4$  ( $x = 0.2, 0.6$  and  $1.0$ ) nanoparticles was calculated using the standard relation given by,

$$\delta = \frac{1}{t^2} \quad \dots 3$$

Where, t is average crystallite size. The values of dislocation density are presented in table 1. The value of dislocation densities are in the range of  $22 \times 10^{14}$  lines/m<sup>2</sup> to  $30 \times 10^{14}$  lines/m<sup>2</sup>.

#### X-ray density ( $d_x$ )

The X-ray density of  $\text{Co}_{1-x}\text{Zn}_x\text{Fe}_2\text{O}_4$  ( $x = 0.2, 0.6$  and  $1.0$ ) nanoparticles was calculated using the standard relation given by equation,

$$d_x = \frac{Z \times M}{V \times N_A} \text{ gm/cm}^3 \quad \dots 4$$

Where, Z is the number of molecules per formula unit ( $Z = 8$  for spinel system), M is molecular mass of the sample,  $V = a^3$  is the unit cell volume,  $N_A$  is the Avogadro's number. The obtained values of X-ray density are presented in table 1. It is evident from table 1 that, the as zinc concentration x increases the X-ray density decreases. The observed decrease in X-ray density can be attributed to the increase in lattice constant.

#### Bulk density ( $d_B$ )

The bulk density of  $\text{Co}_{1-x}\text{Zn}_x\text{Fe}_2\text{O}_4$  ( $x = 0.2, 0.6$  and  $1.0$ ) nanoparticles were determined using Archimedes principle. The values of bulk density are given in table 1. It can be observed from table 1 that bulk density of the present sample was found to be decreased from  $3.61 \text{ gm/cm}^3$  to  $3.44 \text{ gm/cm}^3$ . The observed decrease in bulk density may be due to the decrease in mass. It is also observed that, the values of bulk density of the present samples are quite less than X-ray density which results in high porosity values.

#### Porosity (P)

The percentage porosity of  $\text{Co}_{1-x}\text{Zn}_x\text{Fe}_2\text{O}_4$  ( $x = 0.2, 0.6$  and  $1.0$ ) nanoparticles were calculated from the following relation;

$$P = 1 - \frac{d_B}{d_x} \% \quad \dots 5$$

The obtained values of porosity are listed in table 1, the porosity for the cobalt ferrite sample ( $x = 0.2$ ) is less than that of zinc substituted cobalt ferrite samples ( $x = 0.6$  and  $1.0$ ). The increase in porosity may be due to increase in X-ray density and decrease in bulk density. The high values of porosity (31% to 35%) are attributed to agglomeration of particles during the synthesis procedure.

**Table 1.** Values of Lattice constant (a), X-ray density ( $d_x$ ), Bulk density ( $d_B$ ), Porosity (P), crystallite size (t), dislocation density ( $\delta$ ) for  $\text{Co}_{1-x}\text{Zn}_x\text{Fe}_2\text{O}_4$  ( $x = 0.2, 0.6$  and  $1.0$ ) nanoparticles

Composition	a (nm)	$d_x$ (gm/cm <sup>3</sup> )	$d_B$ (gm/cm <sup>3</sup> )	P (%)	t (nm)	$\delta$ (lines/m <sup>2</sup> )
0.2	8.388	5.310	3.617	31.88	18	30.86E+14
0.6	8.418	5.312	3.537	33.42	20	25.00E+14
1.0	8.440	5.327	3.441	35.41	21	22.67E+14

## Infrared (IR) studies

The room temperature infrared (IR) spectra of  $\text{Co}_{1-x}\text{Zn}_x\text{Fe}_2\text{O}_4$  ( $x = 0.2, 0.6$  and  $1.0$ ) nanoparticles were recorded in the range  $400\text{ cm}^{-1} - 1000\text{ cm}^{-1}$ . The spectra of all the samples are depicted in fig 2 (a-c). It is revealed from the spectra that, two prominent peaks near  $600\text{ cm}^{-1}$  and  $400\text{ cm}^{-1}$  are observed, which are consider to be the typical bands of spinel structure. The higher frequency band  $\nu_1$  and lower frequency band  $\nu_2$  were observed in the range of  $600 - 500\text{ cm}^{-1}$  and  $450 - 380\text{ cm}^{-1}$  respectively and was assigned to tetrahedral (A) and octahedral [B] metal stretching. The values of absorption frequency  $\nu_1$  and  $\nu_2$  are listed in table 2. It is observed from table 2 that the absorption frequency  $\nu_2$  was slightly shifted towards higher frequency and  $\nu_1$  towards lower frequency side with increasing  $\text{Zn}^{2+}$  content. This can be attributed to shifting of  $\text{Fe}^{3+}$  ions towards oxygen ion on the tetrahedral site which decreases with  $\text{Fe}^{3+}\text{-O}^{2-}$  distance. The increase in site radius results in the reduction of fundamental frequency and central frequency which shifts towards the lower side.

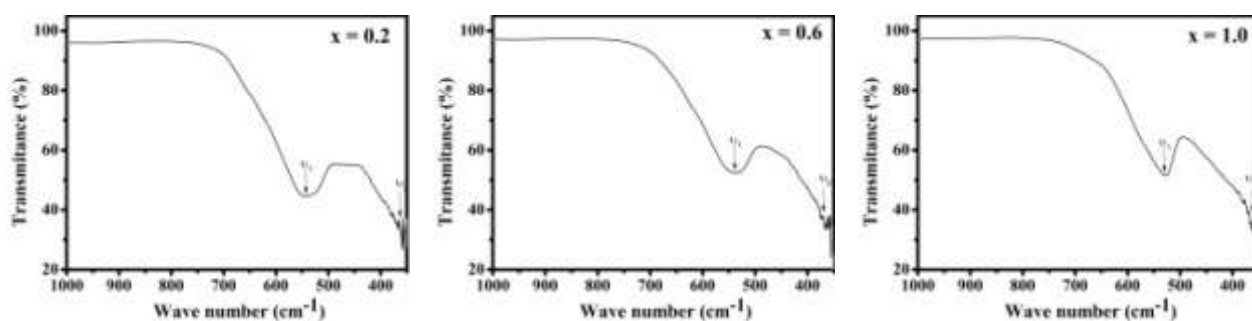


**Fig. 2 (a-c):** IR spectra of  $\text{Co}_{1-x}\text{Zn}_x\text{Fe}_2\text{O}_4$  ( $x = 0.2, 0.6$  and  $1.0$ ) nanoparticles

**Table 2.** Values of infrared absorption frequency band positions ( $\nu_1$  and  $\nu_2$ ) for  $\text{Co}_{1-x}\text{Zn}_x\text{Fe}_2\text{O}_4$  ( $x = 0.2, 0.6$  and  $1.0$ ) nanoparticles

Composition	$\nu_1$ ( $\text{cm}^{-1}$ )	$\nu_2$ ( $\text{cm}^{-1}$ )
0.2	531.39	357.33
0.6	538.23	360.67
1.0	544.15	363.32

## Conclusions

The zinc substituted cobalt ferrite nanoparticles ( $\text{Co}_{1-x}\text{Zn}_x\text{Fe}_2\text{O}_4$  with  $x = 0.2, 0.6$  and  $1.0$ ) were successfully prepared using sol-gel auto combustion method by taking citric acid as fuel. Single phase with cubic spinel structure was observed for all the compositions via the analysis of X-ray diffraction data. Lattice constant found to be increased with zinc substitution  $x$ , which can be attributed to the difference in ionic radii of cobalt and zinc. The average crystallite size obtained through Scherrer's

equation is found in nanometer range which shows the nanocrystalline nature of all the compositions. Infrared spectra showed two absorption bands near  $600\text{ cm}^{-1}$  and  $400\text{ cm}^{-1}$  indicating the characteristics features of cubic structured spinel ferrite nanoparticles.

## References

- [1] A. Mnyusiwalla, A.S. Daar, P.A. Singer, 'Mind the gap': science and ethics in nanotechnology, *Nanotechnology*, 14 (2003) R9.
- [2] F.A. Buot, Mesoscopic physics and nanoelectronics: nanoscience and nanotechnology, *Physics Reports*, 234 (1993) 73-174.
- [3] R. Hiesgen, I. Wehl, E. Aleksandrova, E. Roduner, A. Bauder, K.A. Friedrich, Nanoscale properties of polymer fuel cell materials—A selected review, *International Journal of Energy Research*, 34 (2010) 1223-1238.
- [4] M. Pardavi-Horvath, Microwave applications of soft ferrites, *Journal of Magnetism and Magnetic Materials*, 215 (2000) 171-183.
- [5] I. Sharifi, H. Shokrollahi, S. Amiri, Ferrite-based magnetic nanofluids used in hyperthermia applications, *Journal of Magnetism and Magnetic Materials*, 324 (2012) 903-915.
- [6] A. Sutka, G. Mezinskis, Sol-gel auto-combustion synthesis of spinel-type ferrite nanomaterials, *Frontiers of Materials Science*, 6 (2012) 128-141.
- [7] D.S. Mathew, R.-S. Juang, An overview of the structure and magnetism of spinel ferrite nanoparticles and their synthesis in microemulsions, *Chemical Engineering Journal*, 129 (2007) 51-65.
- [8] K. Maaz, A. Mumtaz, S. Hasanain, A. Ceylan, Synthesis and magnetic properties of cobalt ferrite ( $\text{CoFe}_2\text{O}_4$ ) nanoparticles prepared by wet chemical route, *Journal of Magnetism and Magnetic Materials*, 308 (2007) 289-295.
- [9] N. Somaiah, T.V. Jayaraman, P. Joy, D. Das, Magnetic and magnetoelastic properties of Zn-doped cobalt-ferrites— $\text{CoFe}_2-x\text{Zn}_x\text{O}_4$  ( $x = 0, 0.1, 0.2, \text{ and } 0.3$ ), *Journal of Magnetism and Magnetic Materials*, 324 (2012) 2286-2291.
- [10] S. Singhal, T. Namgyal, S. Bansal, K. Chandra, Effect of Zn substitution on the magnetic properties of cobalt ferrite nano particles prepared via sol-gel route, *Journal of Electromagnetic Analysis and Applications*, 2 (2010) 376.
- [11] N. Sanpo, C.C. Berndt, C. Wen, J. Wang, Transition metal-substituted cobalt ferrite nanoparticles for biomedical applications, *Acta Biomaterialia*, 9 (2013) 5830-5837.